A Comparison between Holographic SAR (HSAR) and Conventional Narrow Angle SAR

Joseph K. Glazner, Donald A. Di Rosa

Houston Advanced Research Center
Senior Research Engineer, RF Sensor Systems Research and Program Development - 4802
Research Forest Drive, The Woodlands, Texas 77381

ABSTRACT

Present day implementations of long wavelength (microwave frequencies) SAR almost exclusively rely on range/Doppler processing techniques. While this has been an effective solution, the implementation necessarily requires a limited data space for processing. This comes from the fact that with conventional SAR the relationship between frequency (cross track dimension) and angle (track dimension) is ignored in the measurement space. This result in the small angle limitation of conventional SAR. If the frequency/angle dependance is not decoupled in Fourier space then the size of the synthesized aperture can be greatly increased and in fact can be 360 degrees.

This paper will discuss the differences in processing between conventional narrow angle SAR and wide angle holographic SAR (HSAR). While many of the differences are subtle some offer significant changes in how one should view the relationship between measurement space and image space, namely the relationship between coordinate systems in both spaces.

Also, differences in output constructs will be presented. Perhaps the most important benefit is the amount and nature of the data that is recoverable with HSAR. These data characteristics, wide angle information, resolution, etc., are best observed by analyzing the data by incrementally increasing the aperture size. This paper will present and discuss just such data.

INTRODUCTION

Conventional SAR processing almost exclusively relies on range/Doppler processing. This processing necessarily requires that data acquisition along the synthetic aperture be restricted to narrow angles. This limiting approximation is the result of the decoupling that the processing assumes between the magnitude of the wavevector and the Fourier angle [Mensa, 1991]. Conventional SAR processes only that information embedded in the scattered signal that is referenced to the sensor's antenna plane (i.e., that portion of the phase associated with relative motion between the scene and the platform).

Holographic SAR (HSAR) processing does not assume that the wavenumber and the Fourier angle are decoupled, in fact the processing treats the Fourier variable as a vector (i.e., the wavevector). By maintaining this Fourier relationship, contrary to conventional SAR processing the narrow integration angle limitation is not invoked. Therefore, holographic processing allows ultra wide integration angles to be possible.

This paper discusses the different assumptions made in SAR and HSAR processing. Presented first is a discussion on the different premisses that each processing technique is based on, particularly the coordinate systems employed by each processing algorithm. Next, a discussion is presented on the effects of integration angle capability for the two different techniques. This discussion is particularly focused on wide integration apertures and what they actually mean in terms of image space information, resolution, fidelity, image information extraction capabilities, etc. Finally, the paper concludes with a discussion on how holographic processing may relax some system design requirements relative to conventional SAR. Discussed are questions on motion compensation, velocity errors, sampling requirements, and the timely availability of 3-D scene information.

1. CONVENTIONAL SAR AND HOLOGRAPHIC SAR PROCESSING

Image reconstruction in the cross-range dimension via Doppler, synthetic aperture, and holographic processing techniques leads to fundamentally similar results because each of these techniques depends on the physical proper-

ties of the scattered fields diffracted from irradiated objects. The angular interval used to observe the signals received from a rotating object for Doppler processing, namely inverse synthetic aperture radar (ISAR), can be considered to form a synthetic aperture which is a circular arc subtending the rotation angle. If the fields observed along this aperture were encoded on a recording medium, the stored information would constitute a hologram [Mensa, 1991].

1.1 SAR Processing

The signal returned from an illuminated object can be expressed as

$$S(t) = A_r \exp [\, 2\pi f (t - \psi(t)) \,] \quad (1)$$

where
A_r is the signal magnitude,
$\psi(t)$ is the spatial phase contribution of the response,
f is the carrier frequency.

Note that equation 1 assumes that the carrier has been mixed out of the returned signal. The second term of equation 1, $\psi(t)$ contributes to the spatial frequency and can be further written as

$$\psi(t) = \frac{2|\overline{R}|}{c} - \frac{2(\hat{v} \cdot \overline{R})\, t}{c\,|\overline{R}|} \quad (2)$$

where,
$\hat{v}$ is the velocity vector of the sensor platform,
$(\hat{v} \cdot \overline{R})$ is the vecot dot product of the platform velocity vector and the range vector.

The first term of equation 2 is that part of the spatial frequency due to the propagation of the electromagnetic wave between sensor and target. The second term is that part of the spatial frequency that is associated with the relative motion between the sensor and the target. This term essentially describes the superimposed Doppler information of the sensed scene.

SAR uses Doppler information to derive the cross-range component in the imaging process. Thus, only the second term in equation 2 is processed while the first term is essentially mixed out of the processed signal. Also, although SAR measurements are made in Fourier space the processing decouples the wavenumber (i.e., wavevector magnitude) and the Fourier angle associated with the wavevector. In fact the Fourier angle is completely ignored in the processing. Instead SAR processes scattered information relative to an angle off boresight of the antenna. That is, Doppler information, is a function of the cosine of the angle, as denoted by the dot product term in equation 2, between the line of sights (LOS) unit vector to a scatterer and the velocity vector of the platform. The LOS vector is the vector from the phase center of sensor's antenna to the scatterer in question. The second term of equation 2, after substitution into equation 1, can be rewritten resulting in the well known expression for Doppler return;

$$f_d = \frac{2\,\overline{V}\cos(\theta)}{\lambda} \quad (3)$$

f_d is the Doppler frequency associated with a scatterer at some angle θ between the platform of the velocity vector and the LOS,
θ is squint angle between the platform velocity and the range vector,
λ is the wavelength of the carrier.

The processing coordinate system is then essentially fixed to the radar antenna since θ is the angle off boresight. This results in the image being referenced to the antenna in such a way that one dimension of the image is truly down range from the antenna and the other dimension is truly cross-range, or orthogonal to the LOS, and parallel to the effective plane of the antenna.

Figure 1 is the coordinate system employed in conventional SAR processing x_a, y_a, z_a are the coordinate axis of the sensor's antenna while x_t, y_t, z_t are the coordinate axes of the target or scene. r_s is the slant range vector and f_d is the Doppler frequency asociated with a scatterer within the illuminated scene. SAR processing assumes that the received informations is referenced to x_a, y_a, z_a axes. The resultant SAR image will then have it's two dimensions corresponding to two orthogonal axes of the SAR antenna. For example, if the radar flies a trajectory that is in the x_a direction then the x_a axis becomes the cross- range dimension of the processed image. This is true for fixed angle side looking SAR and effectively true for squinted systems, since the squint angle is accounted for in the processing. Such systems are spotlight SAR and squinted fixed angle SAR. Likewise, the range dimension of the image corresponds to the line of sight (LOS) of the system, which is orthogonal to the effective antenna plane.

To summarize, the source of cross-range information, using SAR processing, in the reconstructed image is a function of θ, the squint angle to the individual scatterers as shown in equation 1. This angle is referenced to the LOS vector which, because it is orthogonal to the antenna plane references the image processing to the antenna coordinate system. It is important to note that this is the only angular dependence inherent in conventional range/Doppler processing.

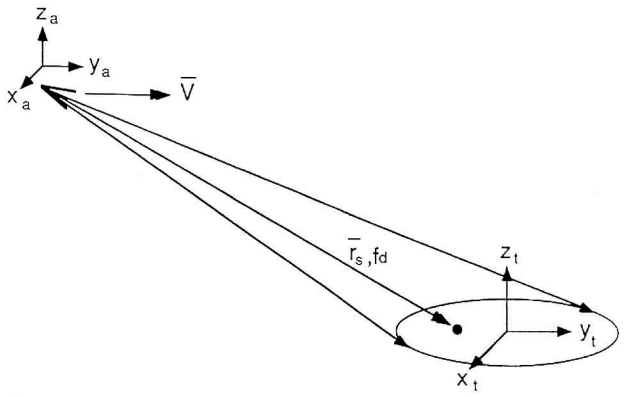

Fig. 1 - Conventional SAR coordinate system.

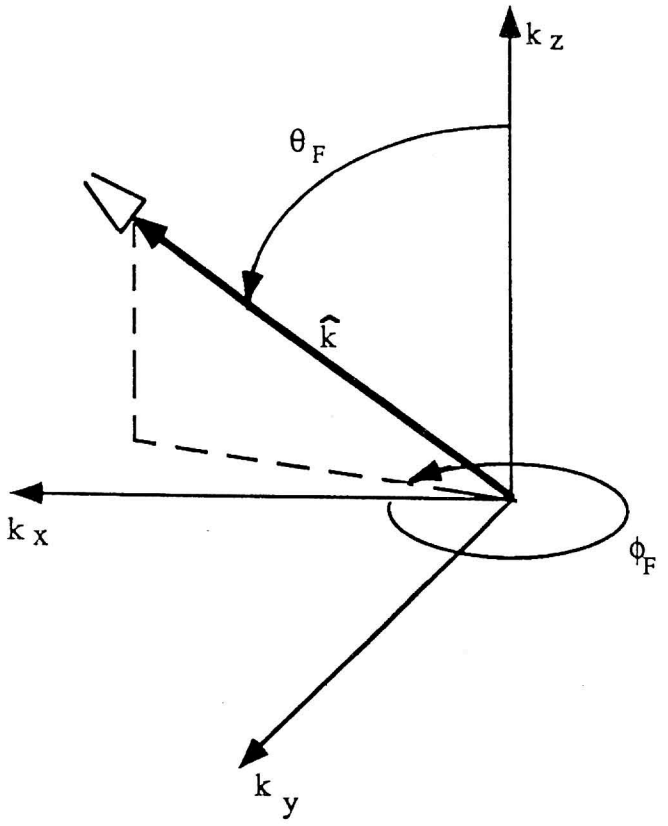

Fig. 2 - Fourier space coordinate system.

1.2 HSAR Processing

HSAR processing is an angle processor. The angle referred to is not the squint angle function discussed above, but rather the Fourier angle. Therefore, the angular synthetic aperture corresponds to the processed angular aperture in Fourier space. This process is described by the first term of equation 2. Substituting equation 2 into equation 1 and considering only the first term of equation 2 results in the following dependence of propagated phase on the wavevector;

$$\psi(t) = 2kR \tag{4}$$

where,

k is the wavenumber.

The above equation can be represented in the more generalized vector form as

$$\psi(t) = 2\,|\,\hat{k}\cdot\bar{R}\,| \tag{4a}$$

The coordinate geometry in Fourier space (frequency domain or k- space) [Schindel, 1989] is shown in figure2. The coordinate system k_x , k_y , k_z describes Fourier space. k is the monostatic wavevector describing the incident and scattered wave. θ_F is the elevation Fourier angle and ϕ_Φ is the azimuthal Fourier angle.

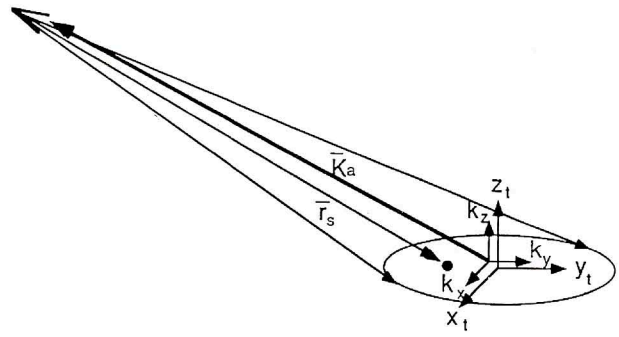

Fig. 3 - Fourier space - spacial space coordinate systems relationship for the particular implementation of HSAR discussed in this paper.

Sensed data is processed relative to the coordinate system in Fourier space. While this coordinate system can be arbitrarily oriented, its origin coincides with the phase center of the sensed scene. The phase center is the reference phase, usually associated with the center of the sensed scene, that each measurement is normalized to. While the origins are collocated it is also convenient to orient the spectral coordinate system so that it is parallel with the spatial space coordinate system of the sensed scene. Figure 3 depicts the relative association between the Fourier space coordinate system and the image spatial space coordinate system assumed in HSAR processing.

The differences in processing coordinate systems employed by SAR and HSAR become apparent in the image reconstruction. Figures 4-8 show the characteristics of image reconstruction using SAR and HSAR processing. Figure 4 is a target array that is used in the processor

simulation to generate the images and to show the differences between SAR and HSAR references. While the assumed system parameters are not important, a comparison of the resultant products are. The array is comprised of point scatterers that are arranged in an arrow fashion. Figure 5-8 show the resultant images from simulation runs performed at HARC. Indicated in the figures are the fixed coordinate system of the target (subscripted t), the reference coordinate system of the image processing (subscripted i), and the coordinate system of the sensor's antenna (subscripted a). Note that in figure 5 and 6, which are images that simulate conventional SAR processing (images are generated by HSAR techniques), the image coordinates and the platform coordinates always coincide and the target orientation depends on the aspect with which it was sensed. The target orientation changes because of the physical relationship between the position of the platform and what constitutes down range and cross-range, relative to the antenna plane, in the images. For example, if the sensor approaches from the direction of the "tail" of the target array, as in figure 5, the tail is near range, the nose is far range, and the target is aligned vertically within the image space, parallel to the LOS and orthogonal to the flight path. (The direction from which the target is flown is discernible from the image by noting that the cross-track resolution is half that of the track resolution.)

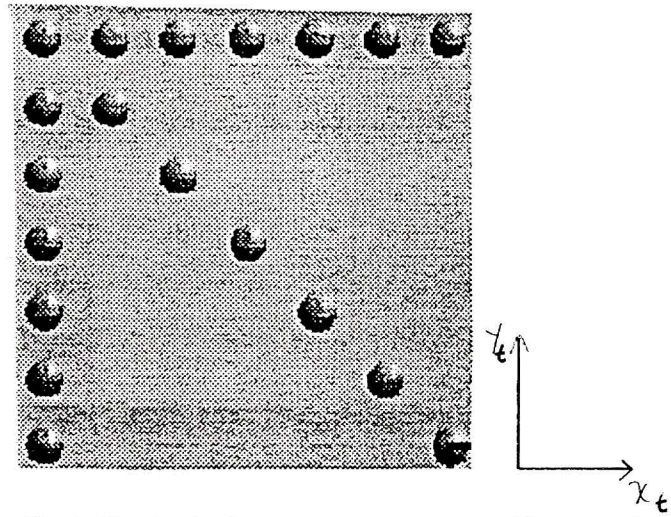

Fig. 4 - Simulated point scatterer target array used for comparison between SAR and HSAR.

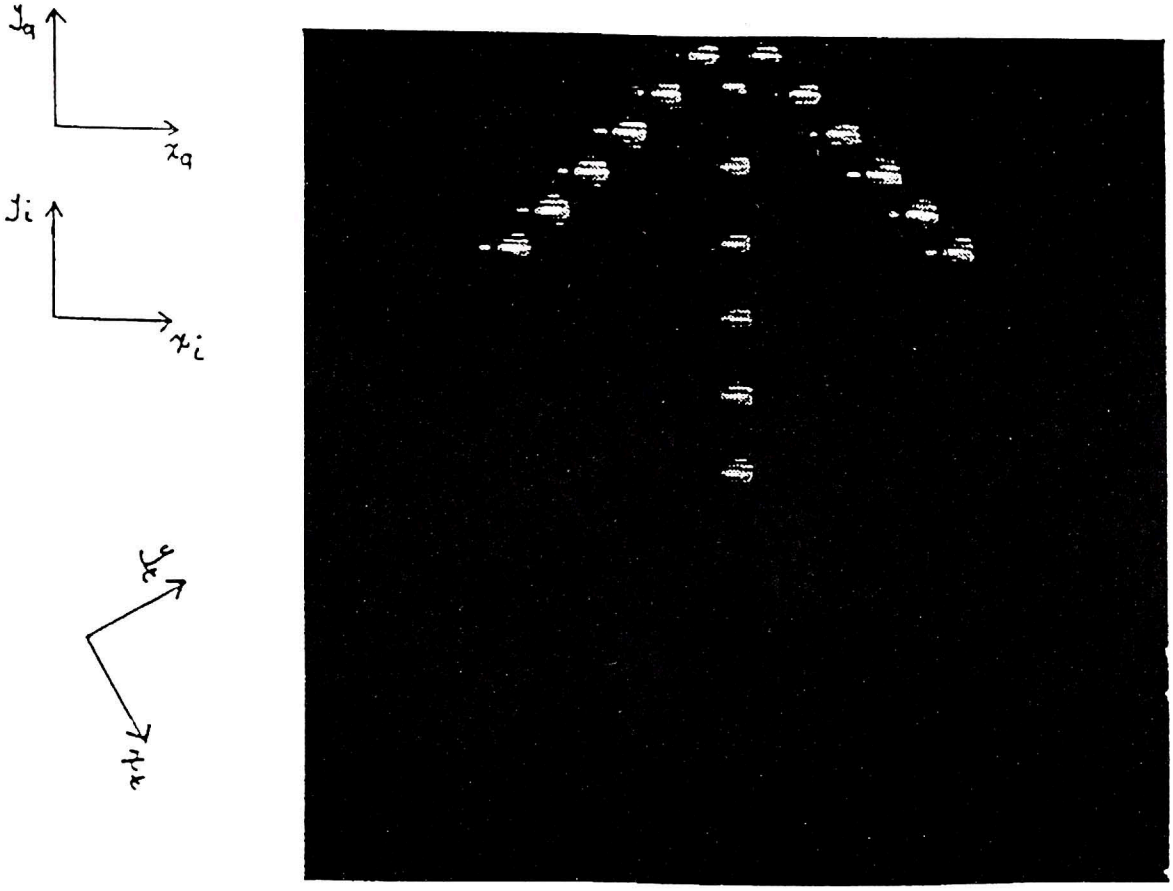

Fig. 5 - Resultant SAR image of target when sensor trajectory is orthogonal to tail of the array.

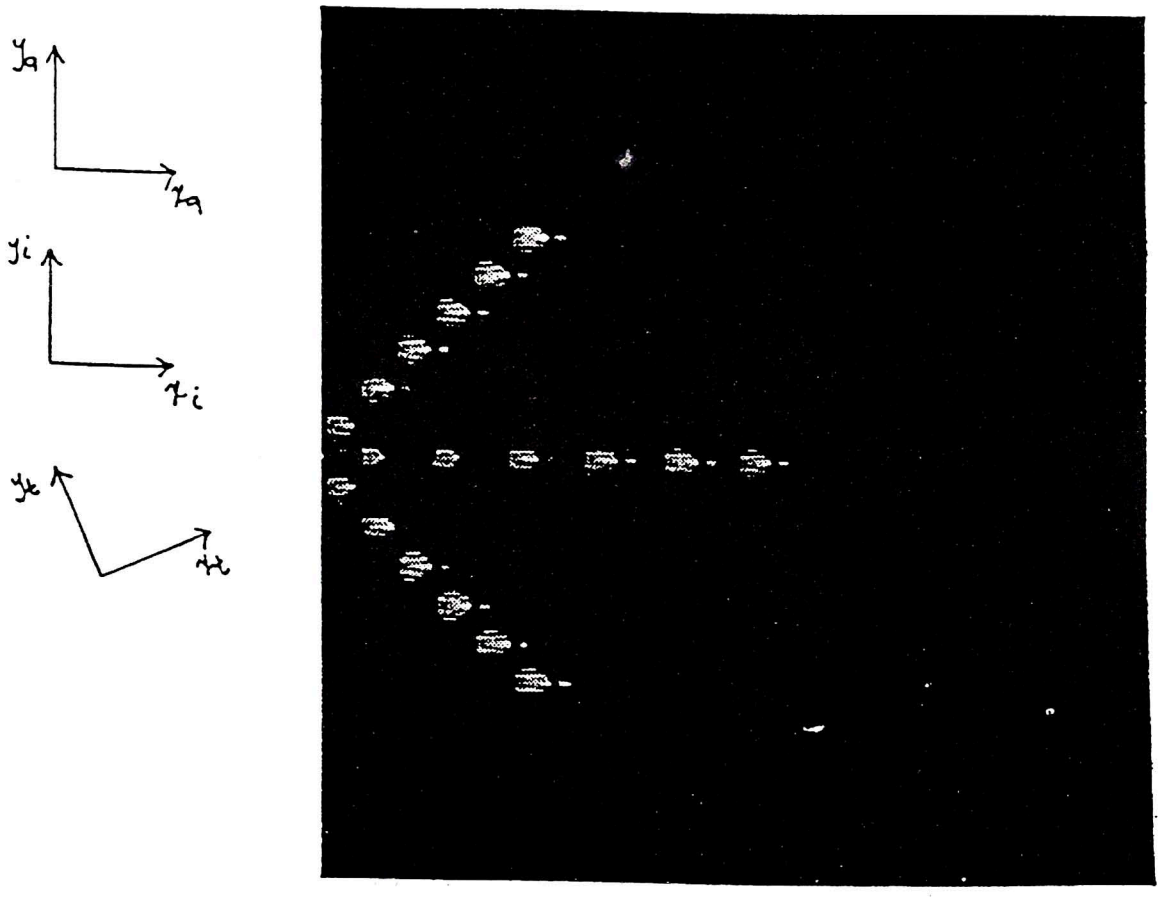

Fig. 6 - Resultant SAR image of target when sensor trajectory is parallel to tail of the array.

Figures 7 and 8 are HSAR images of the same simulated target of figure 4. The simulated flight paths are the same as those flown for the SAR cases. There are significant differences between figures 5 and 6, generated with SAR processing, and figures 7 and 8 generated with HSAR processing. Namely, the target orientation within the image is not a function of the aspect from which the target was observed. For example, the target is approched from the tail-end in figure 7 and from broadside in figure 8, however the target orientation is the same within the image space for both cases. This is true because of the fixed coordinate system assumed in HSAR processing and fact that the Fourier angles where the synthetic aperture samples are made are taken into account. This is in contrast to the SAR processing shown in figures 5 and 6 where target orientation within the image is a function of the observation aspect.

2. WIDE ANGLE PROCESSING

Because SAR sensed information, as discussed above, is referenced to the sensor's antenna it is necessarily limited to narrow angle processing. This is true because as the sensor rotates and observes the target, objects will eventually migrate through more than one resolution cell (Wehner, 1987). This is true of apertures that are significantly larger than the real antenna beamwidth (Ulaby, 1982). While range walk and curvature correction algorithms can minimize this problem, these correction routines are still limited to synthetic apertures on the order of the ground range footprint. The narrow angle restriction has two major implications to the fidelity of conventional SAR processing. First, the achievable cross-range resolution is limited and is usually a fraction of the achievable range resolution which is derived from transmitted band-

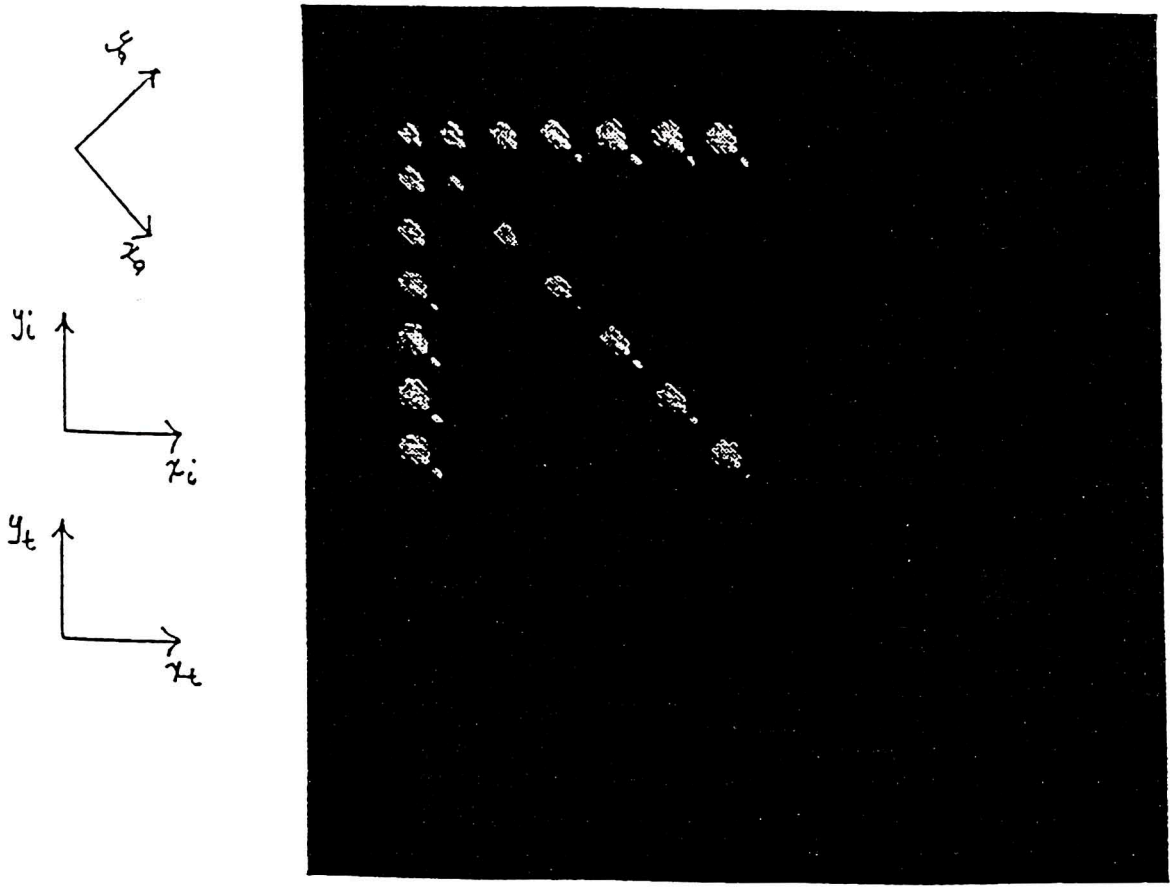

Fig. 7 - Resultant HSAR image of target when sensor trajectory is orthogonal to tail of the array.

width. Second, due to the limited size of the coherent integration angle, scene information is necessarily restricted. This is the result of being able to coherently dwell on the target for only relatively short periods of time. Therefore, in order to observe a scene from all practical viewing aspects several coherent synthetic apertures must be employed and than each resultant coherent image considered independently.

HSAR, because it maintains the Fourier relationship discussed earlier, it is not limited by the narrow angle approximation. Thus, cross-range resolution can be described as approaching the theoretical limit of the point-spread function when observed through 2π radians (Schindel, 1989; Mensa, 1991). The point spread-function, defining the theoretically achievable resolution, of a scatterer located a distance r from the spatial space origin and sensed with N discrete frequencies of $2/\lambda_n$ is given as (Mensa, 1991)

$$h(r) = \sum_{n=1}^{N} \frac{4\pi}{\lambda_n} J_0 \left(\frac{4\pi r}{\lambda_n} \right) \tag{5}$$

where,

J_0 is a zero-order Bessle function.

For a single discrete frequency equation 5 has a peak-to-first null resolution of $\lambda/5$. While this theoretical limit is not realizable for practical considerations such as high integrated sidelobes, it is significantly better than conventional SAR track resolution capabilities defined by equation 6.

$$\Delta r_t = \frac{\lambda}{2\psi_e} \tag{6}$$

Δr_t is the track resolution for convention,
ψ_ε is the coherently integrated synthetic aperture. (Note; is usually on the order of the real antenna aperture size.)

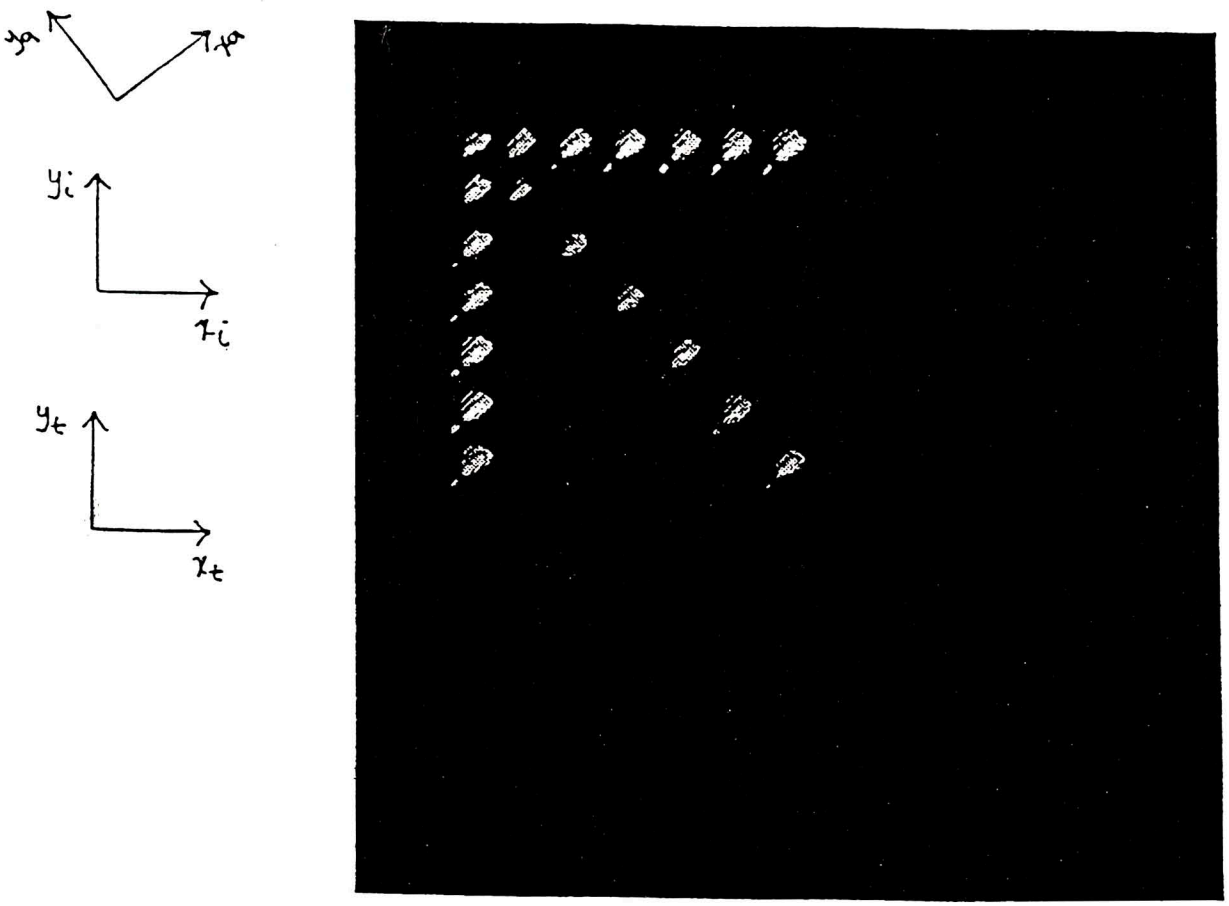

Fig. 8 - Resultant SAR image of target when sensor trajectory is parallel to tail of the array.

The effect of significantly increasing the integrated aperture can be seen in figures 9-13. The left side of figure 9 is the magnitude plot of the sensed wideband spectrum of an aircraft target, irradiated with microwave energy. The right side of the figure is the resultant image. The integrated aperture is approximately five degrees and is consistent with the size of conventional SAR synthetic apertures. As can be seen in the reconstructed image on the right, resolution and target recognizability is poor. Figures 10-13 show the effects of increasing the aperture size. As expected the resolution increases as the aperture is increased from five degrees to 90 degrees. An important point to be made is that conventional SAR is incapable of making measurements much more than a few degrees while HSAR, as seen in figure 13 for example, can process 90 degrees of information.

While the practical implementation of a system might only incorporate an aperture less than 90 degrees, HSAR processing can accomodate 360 degrees of information with a theoretical resolution of that described by the point-spread function of equation 6. Although theoretical resolutions are small fractions of a wavelength, realizable resolutions are much more coarse. This is in part due to integrated sidelobe (ISL) effects (Mensa, 1991) of the point-spread function. ISL levels of -8 dB for unwindowed data are realized in the point-spread function when integrating 360 degrees of information. This fact reduces the observable image resolution of complex target with many scattering sources of comparable amplitude. Dynamic range of wide angle SAR implementations such as HSAR is therefore a legitimate concern.

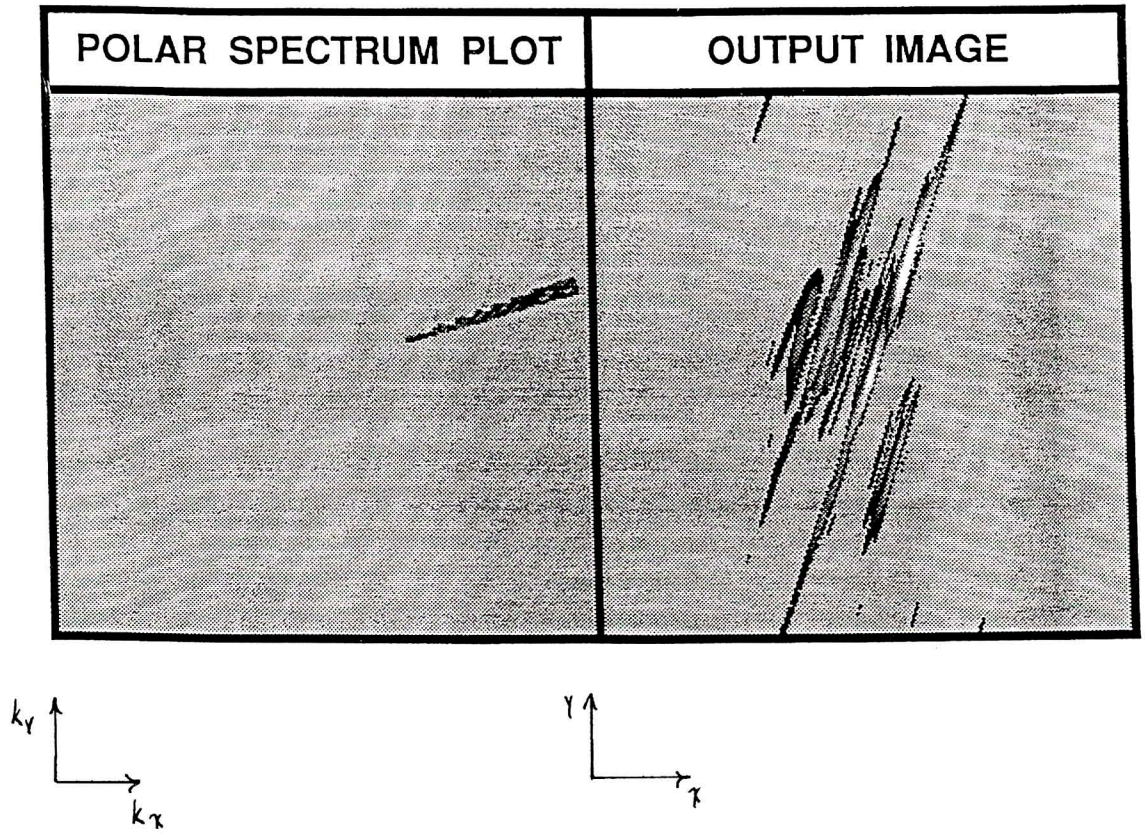

Fig. 9 - Magnitude plot of spectrum and the resultant HSAR image of the of microwave measurements taken of a scaled model aircraft. Aperture is 5 degrees.

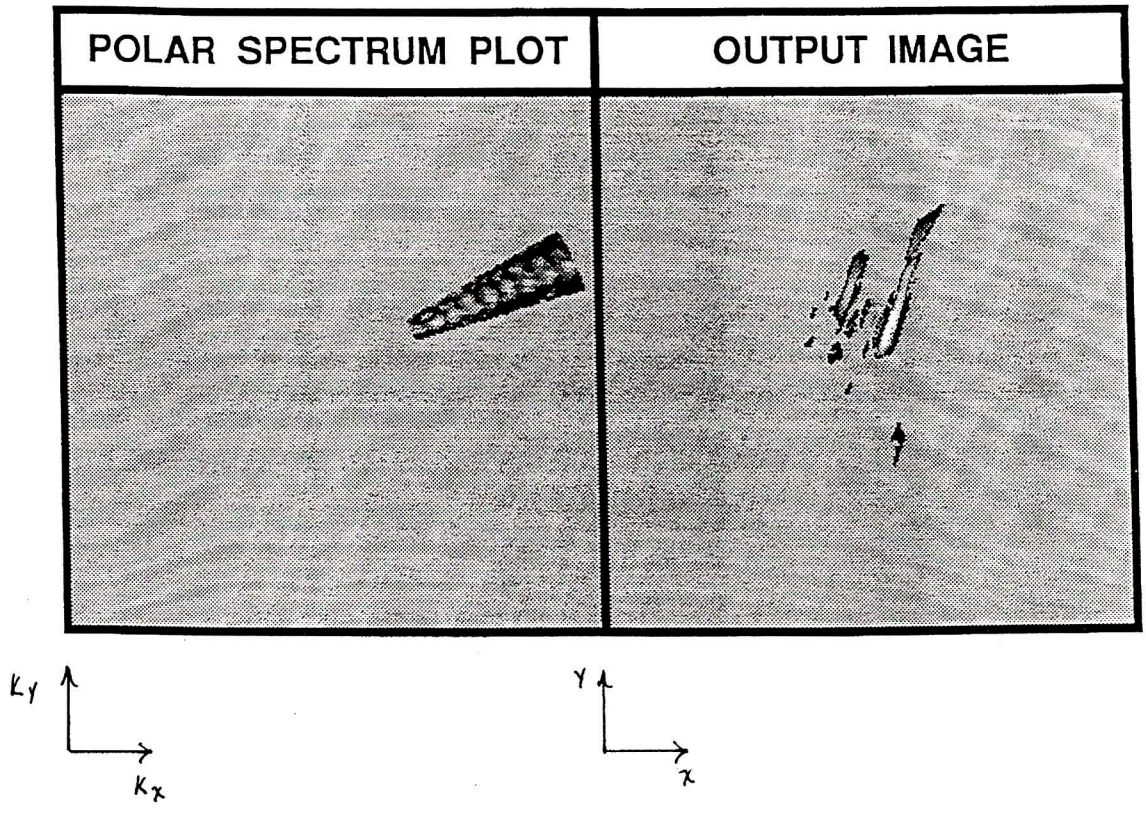

Fig. 10 - Magnitude plot of spectrum and the resultant HSAR image of the of microwave measurements taken of a scalded model aircraft. Aperture is 14 degrees.

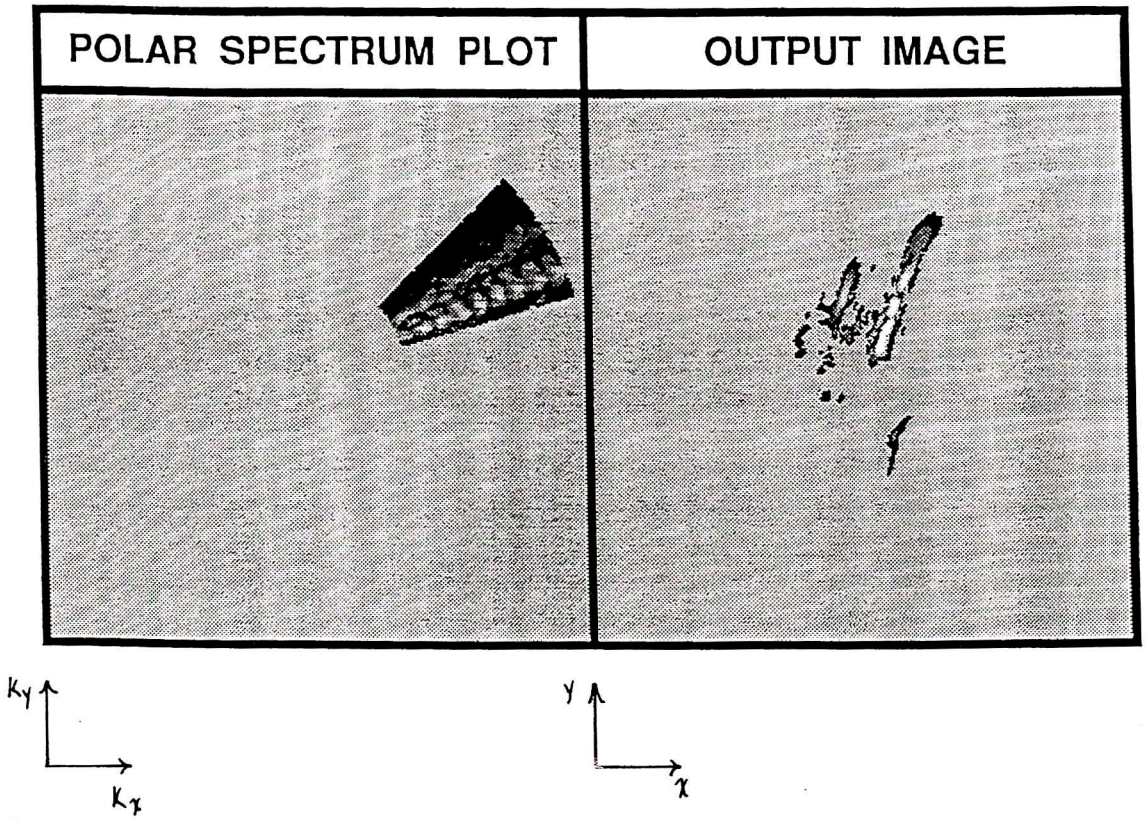

Fig. 11 - Magnitude plot of spectrum and the resultant HSAR image of the of microwave measurements taken of a scaled model aircraft. Aperture is 27 degrees.

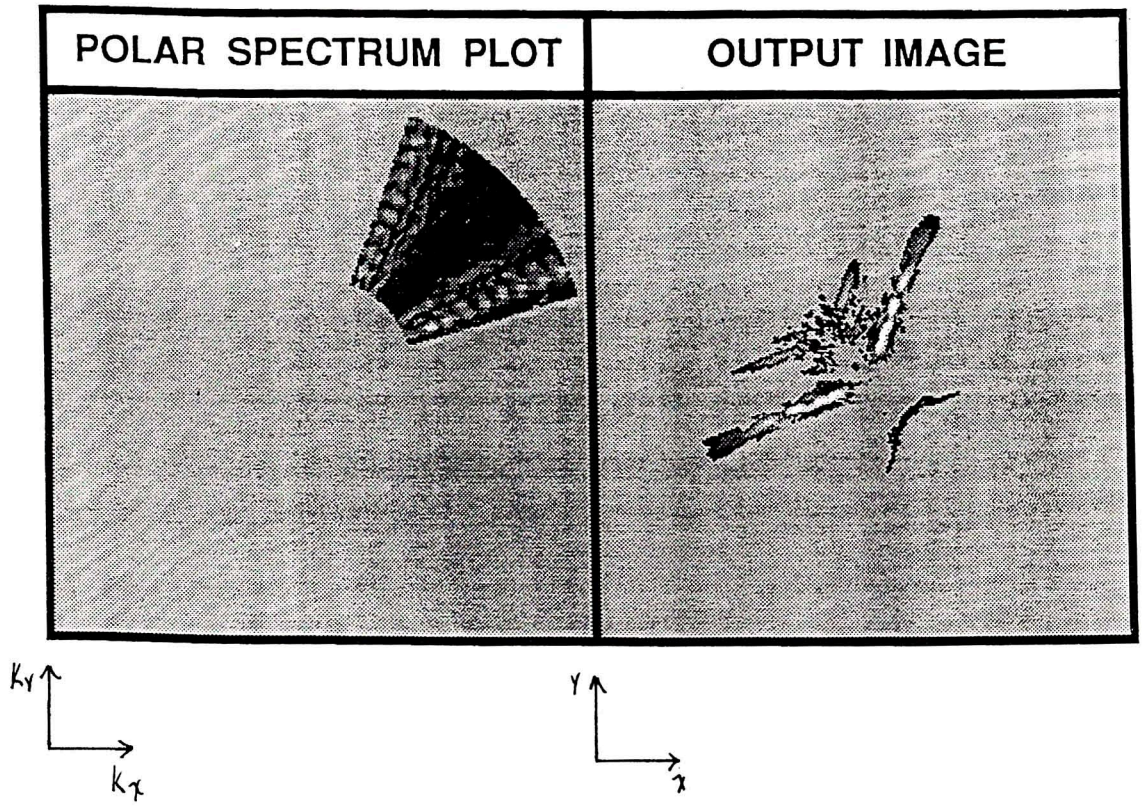

Fig. 12 - Magnitude plot of spectrum and the resultant HSAR image of the of microwave measurements taken of a scaled model aircraft. Aperture is 50 degrees.

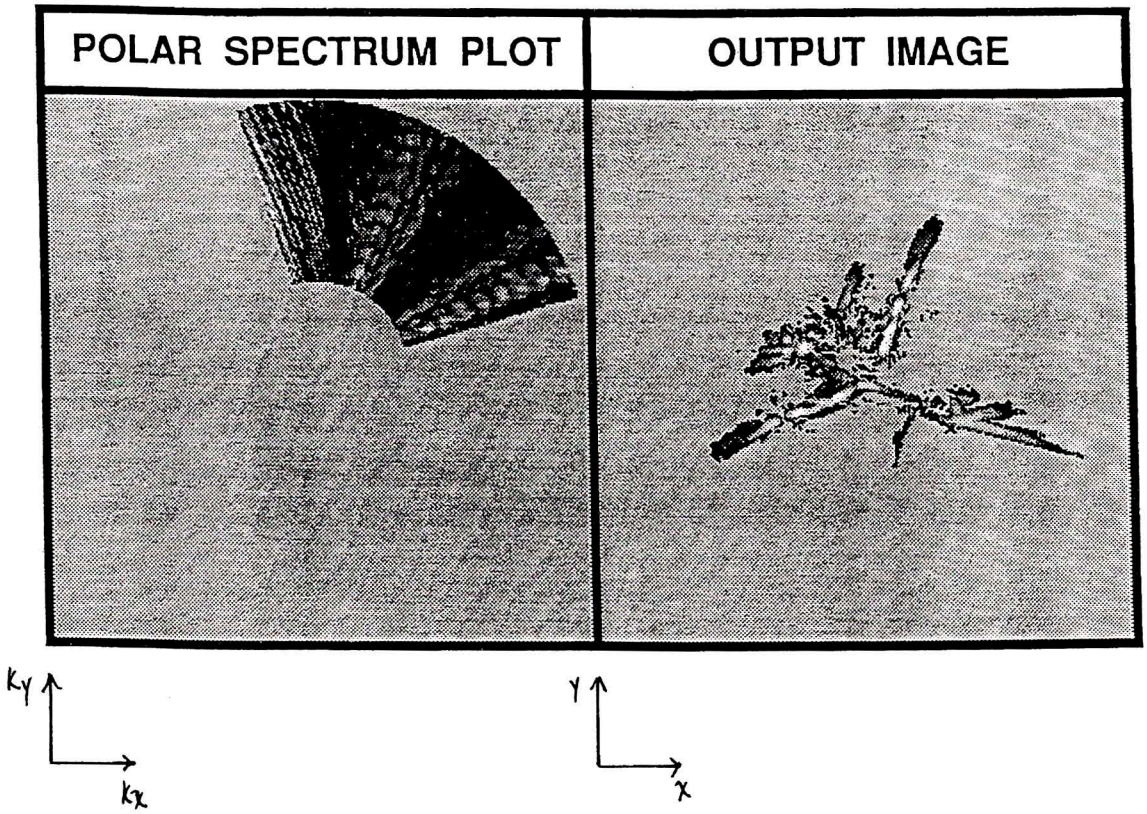

Fig. 13 - Magnitude plot of spectrum and the resultant HSAR image of the of microwave measurements taken of a scaled model aircraft. Aperture is 90 degrees.

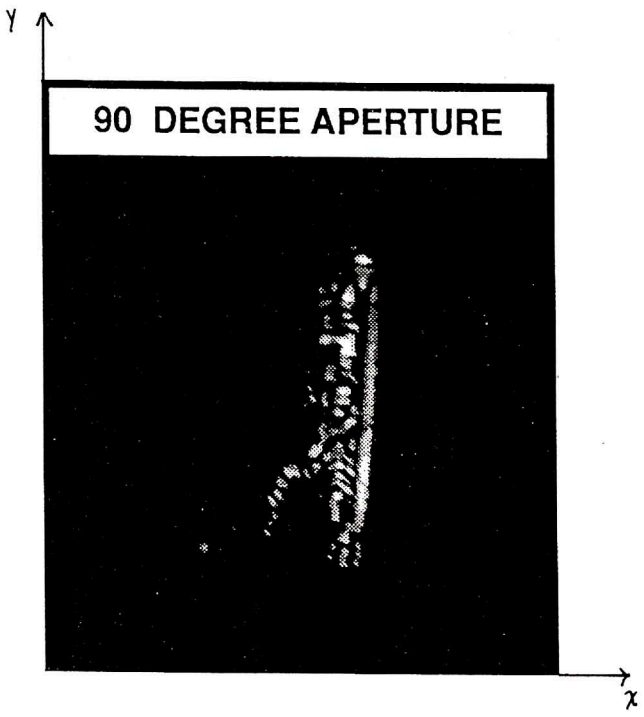

Fig. 14 - Magnitude plot of spectrum and the resultant HSAR image of the of microwave measurements taken of a scaled model tank. Aperture is 90 degrees.

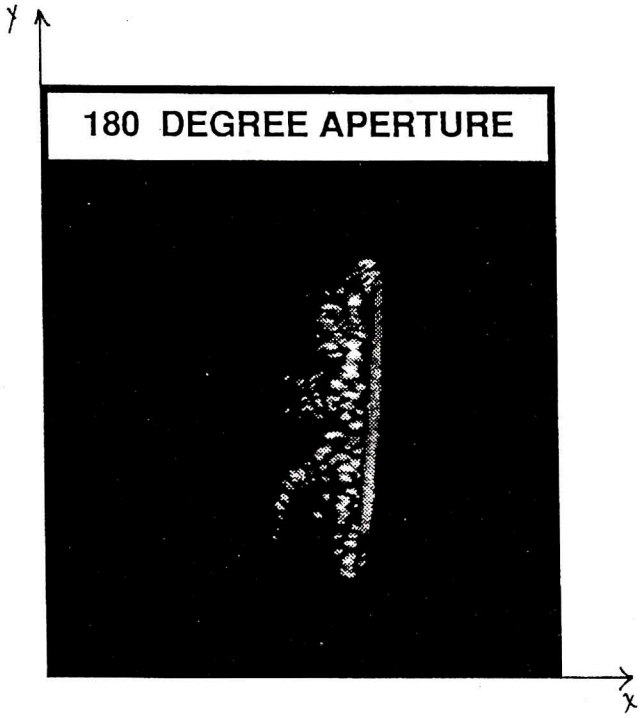

Fig. 15 - Magnitude plot of spectrum and the resultant HSAR image of the of microwave measurements taken of a scaled model tank. Aperture is 180 degrees.

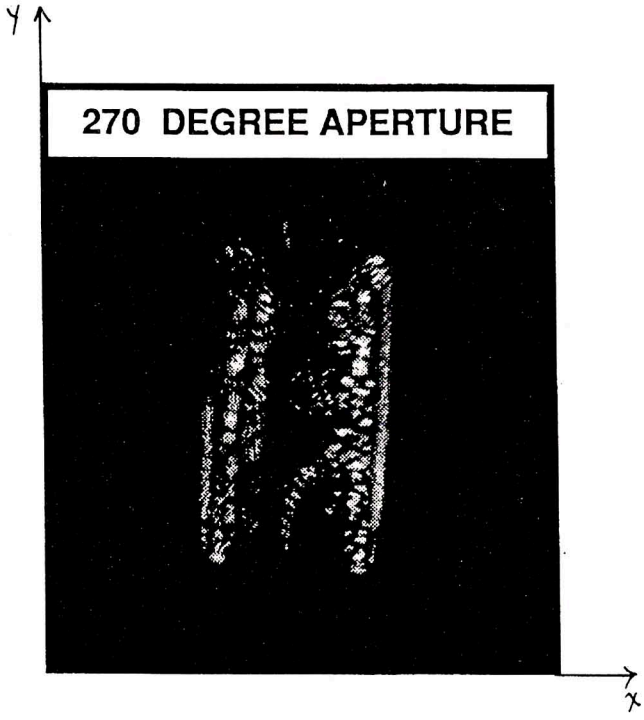

Fig. 16 - Magnitude plot of spectrum and the resultant HSAR image of the of microwave measurements taken of a scaled model tank. Aperture is 270 degrees.

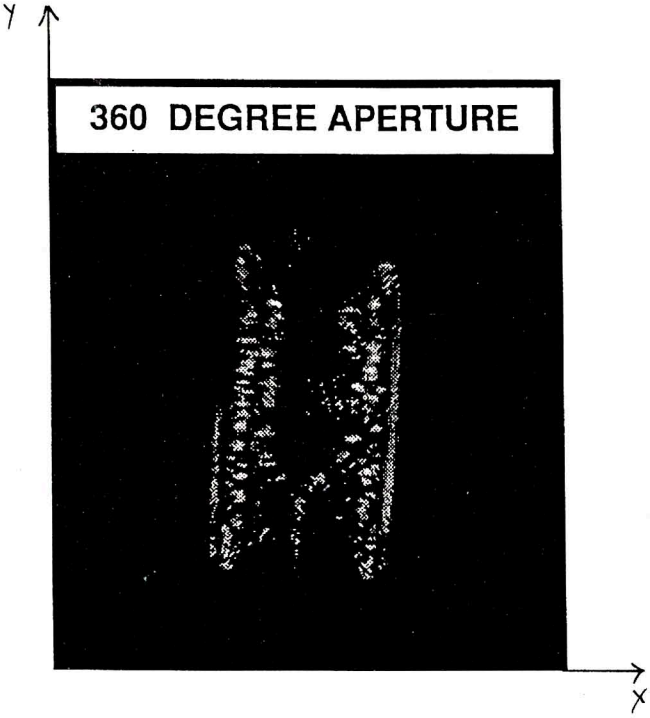

Fig. 17 - Magnitude plot of spectrum and the resultant HSAR image of the of microwave measurements taken of a scaled model tank. Aperture is 360 degrees.

Another contributing factor to achievable resolutions being less than the theoretical limit for complex targets is that while the total object may be observed for some finite angle several scatterers may only be illuminate for a fraction of the total integration period. Thus, the degree to which they are resolved is decreased. Figures 15 - 18 illustrate this point. Figure 14 is an HSAR image of a model tank generated by sensing the target with a wide-band signal and a 90 degree aperture. Figures 15 - 17 are images of the same target sensed with synthetic apertures of 180°, 270°, and 360°. The measurements started at the front of the tank (i.e., the barrel end) and rotated counter-clockwise. Note that while there is an appreciable increase in resolution from 90 degrees to 180 degrees, there is no significant observable difference in resolution between the 180, 270 and 360 degree images. This is true even though resolution is increasing as described by the point-spread function of equation 5. This phenomena is the result of high ISL levels and partial obscuration of indivudual scattering sources during the coherent integration process.

Ultimately, because of ISL levels and obscurations of scatterers during integration, the expressions for track and cross-track resolutions that are often quoted for conventional SAR are good approximations for HSAR processing. For complex targets, increased resolution is not effectively realized for integration angles much greater than 90° which results in a resolution of approximately 0.5 λ. The "granularity" of the image, which is a function of the Fourier processing, is conveniently related to the physical resolution. This is accomplished by choosing grid spacing in the interpolation routine of HSAR processor to be on the order of the incremental wavenumber, Δk (Schindel, 1991)

3. FUNCTIONAL SYSTEM IMPLICATIONS FOR HSAR PROCESSING

There are potentially significant implications to conventional system design when considering an HSAR implementation. These include waveform design (Wehner, 1987), recovery of three dimensional information (Schindel, 1991), and motion compensation. An excellent treatment of waveform considerations is given by Wehner and will not be presented here.

HSAR, by nature of processing, can extract 3-D information by using mutifocal plane techniques (Schindel, 1991), as well as microwave tomographic slice techniques (Schindel, 1989). This is in contrast to conventional 3-D information extraction that use post processing techniques such as shadowing, multiple image registration, etc. One conventional 3-D technique does not use post processing analysis is monopulse image generation. While this is a true 3-D processing technique in the sense that the inherent 3-D information in the measurement data can be extracted in the image reconstruction process. While monopulse SAR has seen limited use, one perceived disadvantage, relative to HSAR, is that the technique is viable for relative short sensing ranges since monopulse performance is range dependent. This would then probably exclude it from remote sensing applications. Figure 18 is a simple depiction of monopulse performance revealing the range dependence. As seen in the figure, the monopulse angle from which sensed information is received must be larger than the width of the monopulse null. At relatively long ranges null coverage is a significant portion of the sensed scene and therefore has limited 3-D capability.

Another significant system implication of HSAR in the area of motion compensation. This is a primary concern in any SAR design, both from a cost stand point, as well as from a technical consideration. Motion compensation requirements may be relaxed for an HSAR system, relative to a SAR system, since HSAR does not process Doppler information. Motion errors, namely velocity errors, degrade SAR system performance because these errors induce additional Doppler frequencies in the scattered signal that are unaccounted for in the processor. HSAR, on the other hand, treats frequency shifts due to Doppler, because they are ignored in the processing, as frequency errors therefore resulting in an unaccounted for chnage in the k vector in Fourier space. This can be illustrated by considering figure 19. Δk in the figure is the incremental change in the wavevector due to a frequency change in the transmitted waveform. For example, with a stepped frequency waveform the change in transmitted frequency from f_1 to f_2 results in a change in the wavevector, in Fourier space, from k_1 to k_2 with the difference being Δk. As in any practical implementation of HSAR, there will be relative motion between the sensor and the scene. This motion superimposes Doppler information on the sensed signal. Part of the Doppler return is the result of the platform flying a predefined trajectory at a predetermined speed. This Doppler information is predictable and is taken into account in the SAR design. Another source of induced Doppler frequency are unpredictable motion errors of the sensor platform. These are not predictable and must be sensed with motion detectors, such as an Inertial Measurement Unit (IMU), and corrected for. As seen in figure 19, the Doppler frequency is essentially a change in the wavevector for a given transmit frequency. This is denoted as $\Delta k + \Delta k_{fd}$, where Δk_{fd} is the additional change in the wavevector due to Doppler effects. For a typical

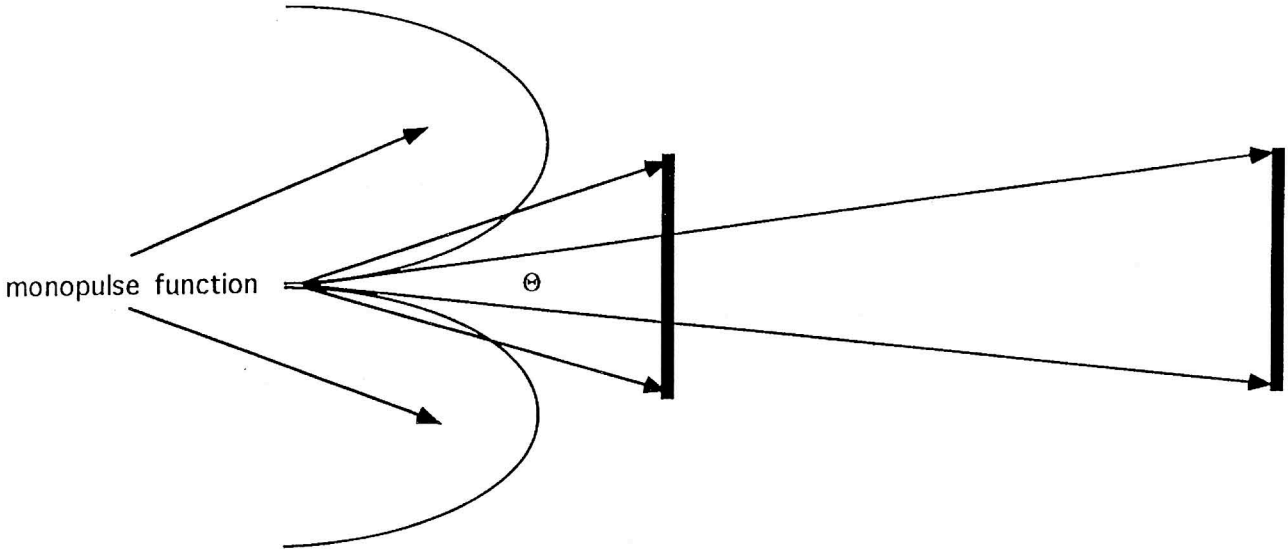

Fig. 18 - Range dependence on monopulse performance.

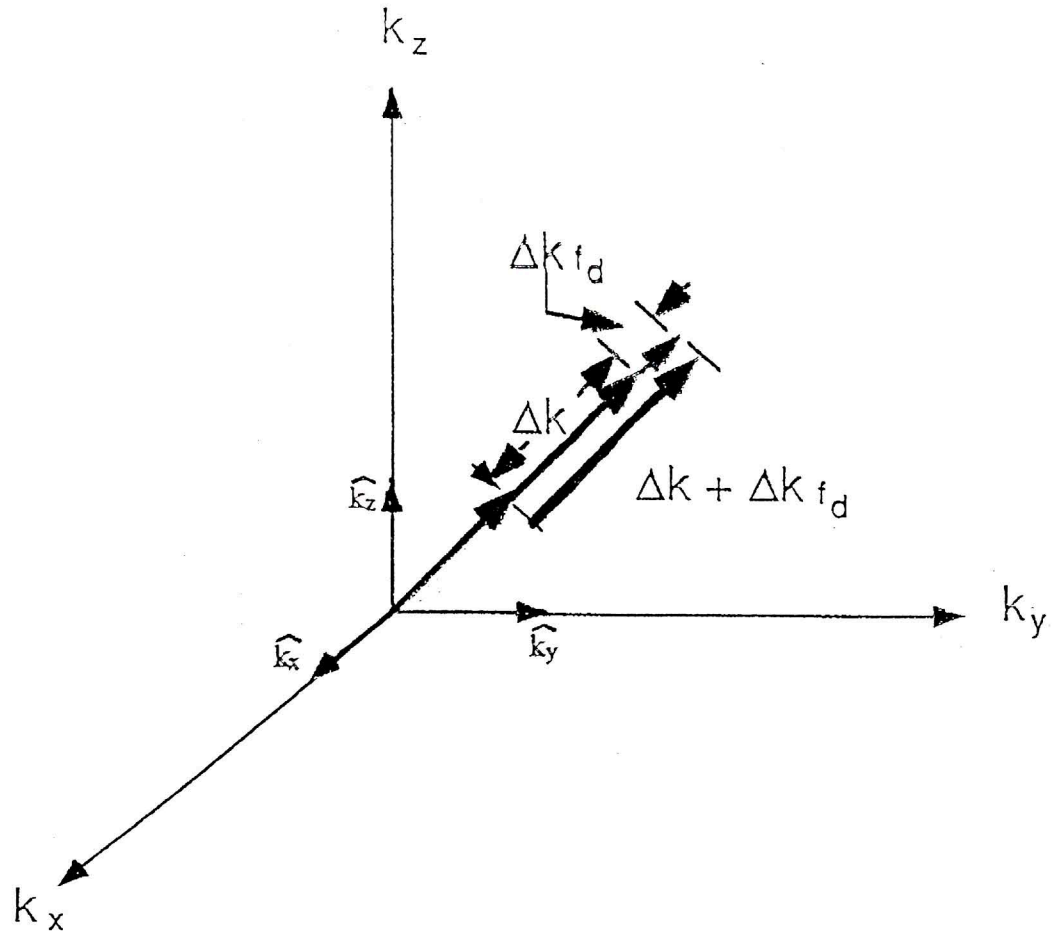

Fig. 19 - Effect of Doppler frequency on the scattered signal.

scene, Doppler information in k-space, Δk_{fd}, would be a relatively small fraction of the incremental wavevector, Δk (e.g., Doppler information is on the order of a few kHz while incremental transmit frequencies are on the order of a few MHz). Simulations have shown HSAR techniques to be exceedingly tolerant of unaccounted for Doppler information within the scene (HARC, 1991).

CONCLUSION

Holographic techniques have been employed in areas such as sonar and optics. While holographic techniques received limited interest in the microwave region in the 1970's and 1980's (Chan, Farhat, 1981), it has only recently received serious attention in the research community (Schindel, 1989). HSAR offers a potentially significant increase in microwave imaging capability. This includes 3-D information extraction both from tomographic processes and multifocal plane techniques, unlimited synthetic aperture sizes, and, potentially, relaxed motion compensation requirements. The combination of these capabilities promises to advance SAR technology that will offer a sensor that can achieve significantly higher resolution at lower frequencies in both two and three dimensions at a lower cost.

REFERENCES

Chan C.K., Farhat N.H., 1981, Frequency Swept Tomographic Imaging of Three-Dimensional Perfectly Conducting Objects, IEEE Transactions on Antennas and Propagation, vol. 29, No. 2.

HARC Internal Report, 1991, Houston, Texas.

Mensa D.L., 1991, High Resolution Radar Cross-Section Imaging Ch. 4 (Boston: Artech House).

Schindel R.F., 1989, Experimental Diverse Microwave Holography, Ph. D. dissertation, The University of Texas at Arlington, Arlington, Texas.

Schindel R.F., 1991, Three Dimensional Aspects of Microwave Holography, European Association of Remote Sensing Laboratories - Workshop on Microwave Imaging and Related Techniques, Alpbach, Austria.

Ulaby F.T., Moore R.K., Fung A.K., 1982, Microwave Remote Sensing - Volume II (Boston: Artech House).

Wehner D.R., 1987, High Resolution Radar (Boston: Artech House).